Introducing nanoresonators into a metal–dielectric–metal waveguide array to allow beam manipulation

Gaige Zheng[1,2]**, Linhua Xu**[1,2]**, Yunyun Chen**[1]**, Yigen Wu**[1] **and Yuzhu Liu**[3]

[1] School of Physics and Optoelectronic Engineering, Nanjing University of Information Science & Technology, Nanjing 210044, Jiangsu, People's Republic of China
[2] Optics and Photonic Technology Laboratory, Nanjing University of Information Science & Technology, Nanjing 210044, People's Republic of China
[3] Paul Scherrer Institute, WSLA-004, Villigen CH5232, Switzerland

E-mail: jsnanophotonics@yahoo.com

Abstract
Stub and circular ring-shaped plasmonic resonators are introduced into a metal–dielectric–metal (MDM) waveguide array to allow light transmission control. Light focusing and splitting effects are verified by the finite difference time domain method; the simulation results reveal that the resonators can be used for modulating the superposition phase of the interference between the surface plasmon wave (SPW) from the end of the resonator and the passing SPW in the waveguide array. Furthermore, a structure utilizing a stub cavity with nonlinear material to control the phase of the transmitted SPW is proposed; the deflection angle of the light can be controlled by means of the intensity of the incident light. The proposed MDM waveguide array with plasmonic resonators, with its compact size, ease of integration, and high output, certainly has potential for application in nanophotonic circuits.

Keywords: light focusing and splitting, surface plasmon waves, metal–dielectric–metal waveguide, optical resonators

(Some figures may appear in colour only in the online journal)

1. Introduction

Plasmonic waveguides have attracted tremendous interest from researchers in recent years due to the potential for guiding and manipulating light at deep subwavelength scales [1–3]. As regards guiding surface plasmon waves (SPWs), different photonic elements with a variety of geometries have been introduced and investigated; examples include metallic nanowires [4], metallic nanoparticle arrays [5], V-shaped grooves [6], metal–dielectric–metal (MDM) waveguides [7–13], and so on. Among these, the MDM waveguide is considered to be a particularly key element in the fields of waveguide couplers [7, 8],

subwavelength scale light confinement [9–11] and integrated optical devices [12, 13].

One of the most interesting areas relating to MDM waveguides, which has been the subject of several recent papers, is the construction of waveguide–cavity systems by side-coupling a stub resonator, consisting of an MDM waveguide of finite length, to an MDM waveguide [14–23]. The MDM waveguide and MDM stub resonators have deep subwavelength widths, so only the fundamental TM mode is propagating. Thus, one can use transmission line theory or scattering matrix theory to account for the behavior of the system. In addition, channel drop filters with disc resonators [24], rectangular geometry resonators [25, 26] and ring resonators [24, 27] have been proposed; the positions of
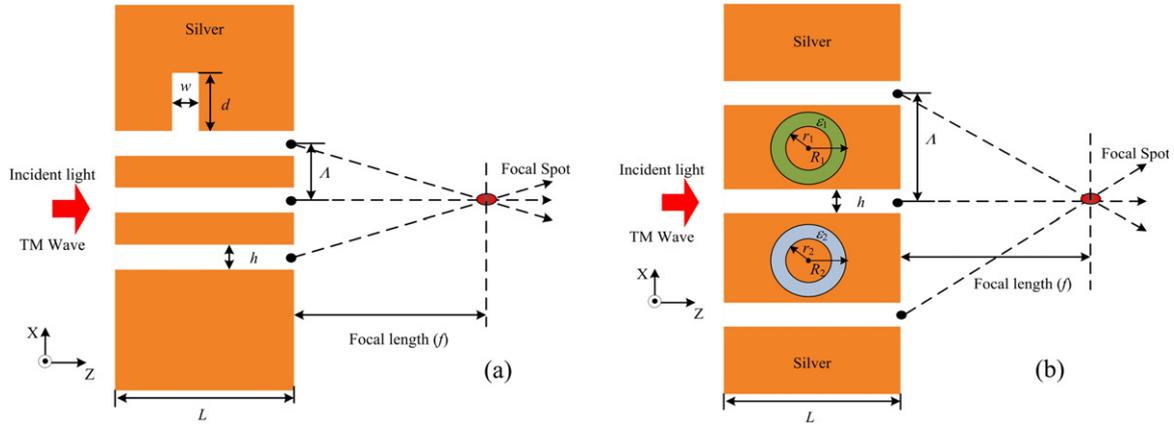
Figure 1. Schematic views of structures in which stub (a) and ring resonators (b) are introduced. The thickness of the structure is L, and the slit interspacing (center to center) is Λ, while each slit width is h. w, d, R_1, R_2, r_1 and r_2 are the width of the stub, the length of the stub, and the outer radii and inner radii of the ring resonators, respectively.

transmission peaks can be easily modulated by changing the parameters of the ring, and thus the aforementioned structures can be used in band-pass and stop-band filters.

Recently, positional modulation through use of a metallic slit array was demonstrated numerically and experimentally [28–30]. In this paper, we extend the previous studies and examine ways of controlling the phase front of the transmitted beam by introducing stubs and circular ring-shaped resonators. The position of the constructive interferences of the decoupled EM waves transmitted through the MDM waveguide array depends strongly on the phase delay profile, and is expressed as a beam modulation effect. With different combinations, multi-beam splitting has been demonstrated through numerical calculation. When the resonator is filled with nonlinear material, the radiation direction and focal length can be changed by varying the intensity of the incident light. Making the appropriate choice of parameters, the proposed structure can be fabricated by focused ion beam (FIB) techniques and there is no need to change the period of the array, or the length and width of the slits.

2. Structures and the simulation method

The MDM waveguide with resonators is shown schematically in figure 1; it consists of a linear array of three air-filled rectangular slits in a silver (Ag) background. The thickness of the structure is L, and the slit interspacing (center to center) is Λ, while each slit width is h. A single stub of width w and length d is coupled with one of the air slits, which can be seen in figure 1(a). In figure 1(b), two ring resonators with outer radii R_1, R_2 and inner radii r_1, r_2 are introduced. The ring resonator can be filled with different dielectric materials. A TM-polarized plane wave with the wavelength of 633 nm illuminates to the slit array normally, from the left side.

In the calculation, the dielectric function of Ag is described by the Drude model as follows:

$$\varepsilon_{Ag}(\omega) = \varepsilon_\infty - \frac{\omega_p^2}{\omega^2 + i\gamma\omega} \qquad (1)$$

where ε_∞ is the infinite frequency dielectric constant, ω_p is the bulk plasma frequency, ω is the angular frequency, and γ is the collision frequency which is related to the dissipation loss in the metal. These parameters are set to 6.0, 1.5×10^{16} rad s^{-1} and 7.73×10^{13} rad s^{-1}, respectively [31]. We assume monochromatic operation with the free space wavenumber $k_0 = \omega_0/c$, the time dependence of $\exp(-i\omega t)$, and the corresponding free space wavelength $\lambda_0 = 2\pi/k_0$. Here, c is the speed of light in vacuum.

To demonstrate the validity of the designed structure, a two-dimensional finite difference time domain (FDTD) simulation is performed with perfectly matched layer (PML) absorbing boundary conditions in the x and z directions of the simulation domain. Since the width of the bus waveguide is much smaller than the operating wavelength in the structure, only the fundamental waveguide mode is supported. The incident light for excitation of the SPP mode is a TM-polarized (the magnetic field is parallel to the y axis) fundamental mode. In the following FDTD simulations, the grid sizes in the x and z directions are chosen to be $\Delta x = \Delta z = 2$ nm and $\Delta t = \Delta x/2c$, which are sufficient for numerical convergence. The normalized time-averaged magnetic field intensity $|H_y|^2$ is employed to represent the field intensity.

3. Phase modulation of transmitted light with stubs

When incident light illuminates the left side of the structure, the wave is coupled to surface plasmon polariton (SPP) modes at the entrances of the metallic slits and propagates along the slits. After transferring to the ends of the metallic slits, the SPPs will be converted to radiating fields due to the scattering of the structure surface. There are two SPP modes in the metallic slit, which are the symmetric mode and the anti-symmetric mode with its H-field distributions. In the subwavelength slit, only the symmetric mode exists, and the anti-symmetric mode undergoes cutoff. Utilizing Maxwell's equations and the boundary conditions, the complex propagation constant β of the fundamental SPP
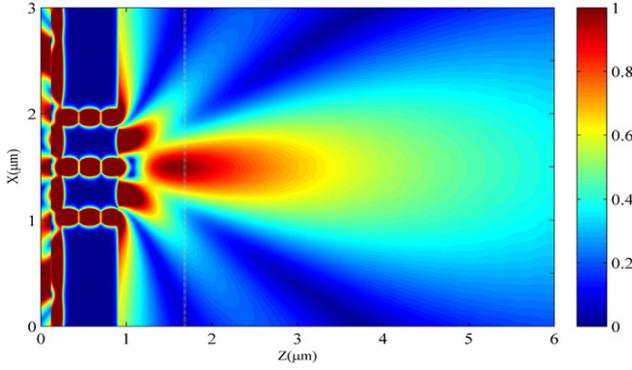
Figure 2. Intensity distribution of focused light for the focal length of 0.69 μm with three slits filled with air. $L = 670$ nm, $\Lambda = 470$ nm, $h = 100$ nm are chosen in the calculation.
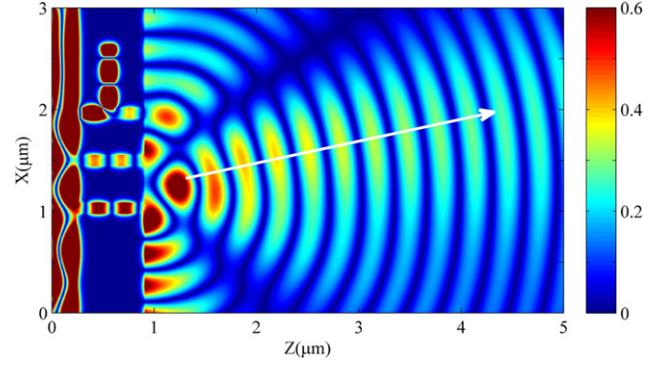
Figure 3. Beam deflection by the nanoslit array lens at fixed $d = 600$ nm, $w = 100$ nm; the other parameters are the same as in figure 2.

mode is given by the following equation [32]:

$$\tanh\left(\frac{h}{2}\sqrt{\beta^2 - \varepsilon_d k_0^2}\right) = \frac{-\varepsilon_d \sqrt{\beta^2 - \varepsilon_{Ag} k_0^2}}{\varepsilon_{Ag}\sqrt{\beta^2 - \varepsilon_d k_0^2}} \quad (2)$$

where $k_0 = 2\pi/\lambda$ is the wavevector of the incident light. ε_d and ε_{Ag} are relative dielectric constants for metal and the materials between the slits, respectively. The effective index n_{eff} of the MDM waveguide as a function of wavelength can be solved from $n_{eff} = \beta/k_0$. We know that the complex wavenumber gradually decreases as the slit width increases. If the slit width goes to infinity, β approaches the propagation constant in the air [24, 28, 32].

In the three-slit-based planar MDM waveguide, each radiating field at the ends of metallic slits can be regarded as an individual point source, while the propagation is in the shape of spherical waves from the sources into the air; they are focused at a specific point due to the constructive interference. Figure 2 shows the intensity distribution under this condition with the focal length f of 0.69 μm and the full width at half-maximum (FWHM) of 438 nm. The simulation parameters are chosen as $L = 670$ nm, $\Lambda = 470$ nm, $h = 100$ nm.

In two-dimensional structures, a stub is considered as a finite MDM waveguide terminated by metal. The main characteristic of stub structures is wavelength filtering. They are coupled to the MDM waveguide perpendicularly or longitudinally. The SPPs excited along the surface of the metal layers propagate in the waveguide with a resonance mode. On passing through the stub, parts of the SPPs propagate into the side-coupled stub. The SPPs reflected from the end of the stub interfere with the passing SPPs, which leads to a modulation of the superposition wave. As shown in figure 3, when a single stub with $d = 600$ nm and $w = 100$ nm is coupled to the top slit, the deflection angle of the main beam is observed to be around 10° and the magnetic field amplitude of the focused beam is a little bit lower as compared to that for the flat case (figure 2). As seen from figure 3, the design varies not only in bending angle, but also in light distribution and intensity in the slits.

The numerical values of the magnetic field verify that different beam splitting effects can be achieved by simply

changing the stubs, as shown in figure 4. Recently, beam splitting in metallic nanostructures has been seen to offer the chance of designing ultracompact splitters [33, 34]. However, the structure is usually very complex. In this work, we propose a simple system consisting of an MDM waveguide array and stubs for beam splitting use. With different combinations, multi-beam splittings are demonstrated. Figure 4(a) reveals that one input beam can be split into two beams with the same intensity. In a similar way, as shown in figure 4(b), under the proper choice of the stubs, the designed structure can produce three beams.

4. A plasmonic lens with a circular ring resonator

There are myriad possibilities for coupling the electromagnetic field of a plasmonic waveguide into a resonator, and thereby spurring either a peak or a dip in the transmission coefficient of the waveguide, to realize wavelength filtering; plasmonic waveguide resonators are by and large formed with MDM arrangements. When two ring resonators are coupled to the metal slit, the focal length and the FWHM of the focal spot can be adjusted accordingly. Figure 5 shows representative simulation results for the plasmonic lens. From the figure, a clear-cut focus appears about 0.598 μm away from the exit plane. The cross-section of the focal spot in the x direction is given in figure 5(b), indicating a FWHM of 424 nm. In this model, $R_1 = R_2 = 125$ nm, $r_1 = r_2 = 25$ nm, and $\varepsilon_1 = \varepsilon_2 = 1$; the other parameters are the same as in figure 2.

When the symmetry of the structure is destroyed, the transmitted light will be bent because of the different phase changes through the slits. We can build an asymmetric phase front across the plasmonic lens to achieve directional modulation by changing the parameters of the resonators. Figure 6 shows two different proposals for this case: in figure 6(a), only one ring resonator is introduced, and in figure 6(b), the two resonators are filled with different materials. By introducing asymmetrical resonators, we can create a relative phase difference profile across the width of the lens (x axis). It is should be pointed out that the proposed lenses can be conveniently fabricated using focused ion beam (FIB) techniques and are thus much more compact and convenient than their existing counterparts.
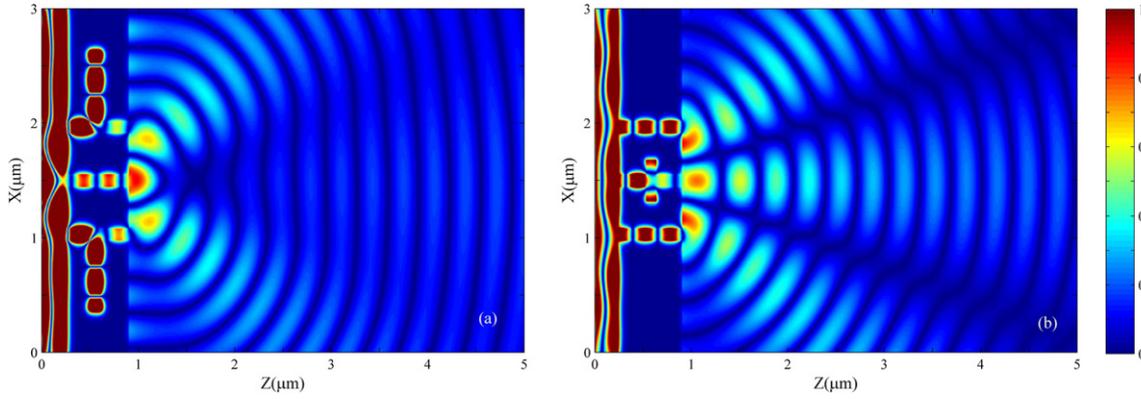
Figure 4. The calculated magnetic field of the designed beam manipulation device for the beam splitters to produce two and three beams. (a) The parameters of the double stubs are the same as in figure 3. (b) A single stub is coupled to the central slit with $d = 351$ nm, $w = 100$ nm.
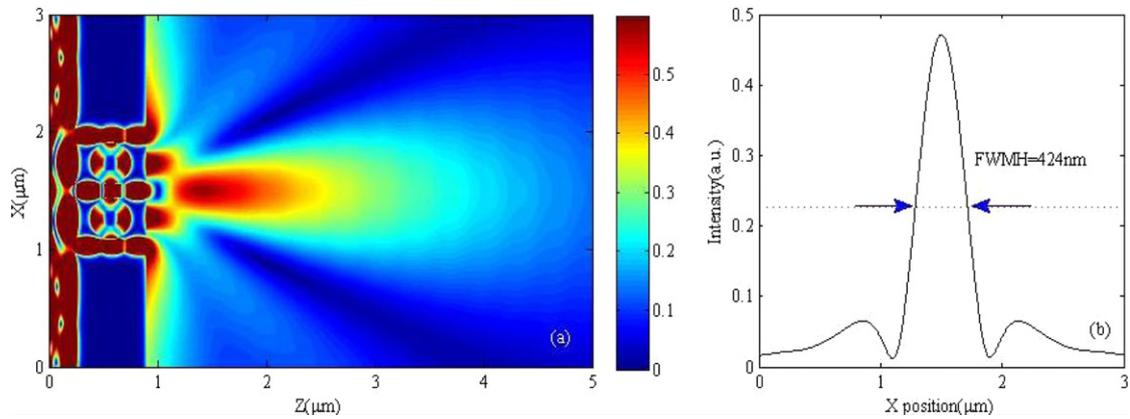
Figure 5. (a) The field intensity distribution of the light transmitted through the plasmonic structure with two ring resonators. (b) The cross-section at the focal point along the *x* axis.
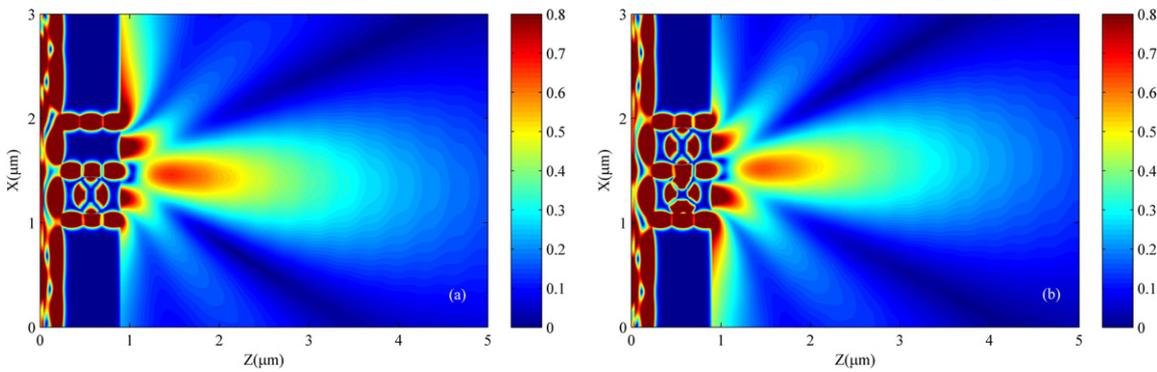

Figure 6. (a) and (b) show two representative designs of plasmonic lenses with different bending angles. In (a), a single ring resonator is introduced; in (b), $R_1 = R_2 = 125$ nm, $r_1 = r_2 = 25$ nm, and $\varepsilon_1 = 1$, $\varepsilon_2 = 2$; the other parameters are the same as in figure 5.

5. Beam deflection with stubs filled with nonlinear material

Recently, nonlinear optical devices based on subwavelength metallic structures have been proposed for the active control of plasmonic signals [35–39]. Asanka presented approximate analytical expressions describing the optical bistability phenomenon in a nonlinear device based on a plasmonic gap waveguide. The device is formed from an MDM waveguide perpendicularly coupled to a stub structure that is filled with an optically nonlinear medium [40]. It is not the focus of our discussion on the transmission spectrum of the stubs coupled to MDM waveguides. We assume that the intensity-dependent index change in the stub is completely governed by the third-order optical nonlinearity of the material. The subwavelength slit is coupled to one stub
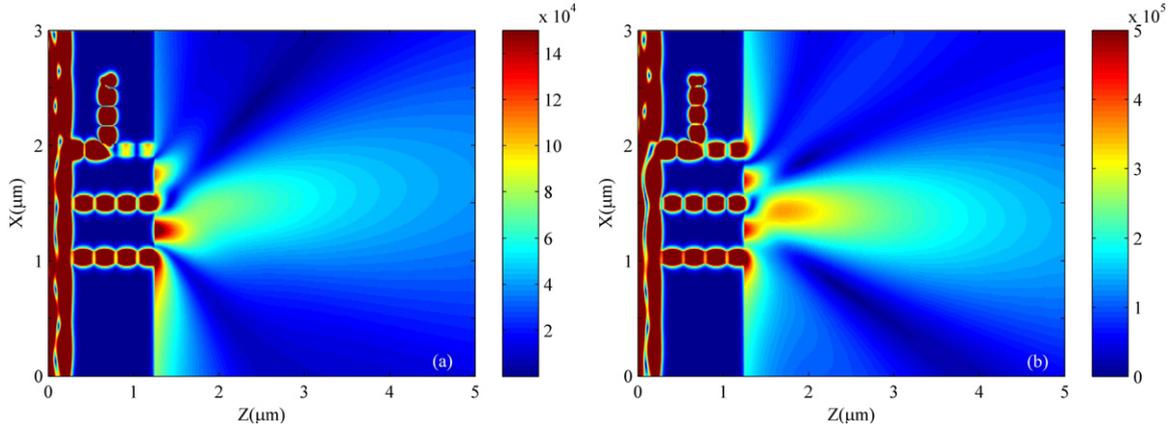
Figure 7. Magnetic field intensity distributions at different incident intensities when the stub is filled with a Kerr nonlinear medium: (a) $|E|^2 = 1 \times 10^{16}$ V^2 m^{-2}; (b) $|E|^2 = 9 \times 10^{18}$ V^2 m^{-2}. The other parameters are the same as in figure 3.

filled with a Kerr medium whose dielectric constant depends on the intensity of the incident light [37, 39]:

$$\varepsilon_d = \varepsilon_L + \chi^{(3)}|E|^2 \tag{3}$$

where ε_L is the linear dielectric constant and set as 2.25, and the third-order nonlinear susceptibility $\chi^{(3)}$ is chosen as a typical value for nonlinear optical materials such as InGaAsP, that is $\chi^{(3)} = 1 \times 10^{-18}$ m^2 V^{-2} ($\approx 1.4 \times 10^{-10}$ esu). The auxiliary differential equation (ADE) method is used to simulate dispersive media in a FDTD calculation. To simulate the performance of our proposed devices, we have solved Maxwell's equations and imported a nonlinear polarization vector into our program:

$$\begin{aligned} \nabla \times \mathbf{E} &= -\mu\frac{\partial}{\partial t}\mathbf{H} \\ \nabla \times \mathbf{H} &= \frac{\partial}{\partial t}\mathbf{D} \\ \mathbf{D} &= \varepsilon_0\varepsilon_\infty\mathbf{E} + \mathbf{P}_L + \mathbf{P}_{NL} \end{aligned} \tag{4}$$

where ε_0 is the free space permittivity, and $\mathbf{P}_L$ and $\mathbf{P}_{NL}$ are the linear and nonlinear polarization vectors related to the Drude model and Kerr nonlinearity, respectively:

$$\begin{aligned} \frac{\partial^2\mathbf{P}_L}{\partial t^2} + \gamma_p\frac{\partial\mathbf{P}_L}{\partial t} &= \varepsilon_0\omega_p^2\mathbf{E} \\ \mathbf{P}_{NL} &= \varepsilon_0\chi^{(3)}\mathbf{E}^3. \end{aligned} \tag{5}$$

The optical intensity is determined by $|E|^2$, which represents the amplitude (peak value) of the incident light; $|E|^2$ is chosen as 1×10^{16} V^2 m^{-2} and 9×10^{16} V^2 m^{-2}. FDTD simulations of the magnetic field distribution at different incident intensities are shown in figures 5(a) and 7(b). By changing the intensity of the incident light, the focal length, the FWHM of the focal width and the bending angle can be adjusted. This relation implies a way of achieving focusing modulation by changing the dielectric constant in the metallic slits, which can be implemented by embedding nonlinear material into the slits.

Multiple slits have been used to yield beams [28–30, 32]. The phase of the components of the field radiating from the multiple slits can be controlled by adjusting the width

of the slits or the refractive index of the material filling the slits. However, it is not easy to dynamically change or tune the beam characteristics using these techniques. In our research, a method for manipulating the beam through three subwavelength metal slits coupled with a dielectric resonator is proposed. Controlling the focus by using the incident light should also prove very useful in potential practical applications.

Both the stub waveguide and the ring resonator can provide wavelength filtering and phase modulation. For ultracompact higher order optical filters, ring resonators are much better because of the narrower bandwidth as compared with that of the stub-based structure. Using MDM waveguides, resonators with very short round trip length can be realized, which is preferable for plasmonic ring resonators due to a lower propagation loss inside the resonator. In addition, a short round trip length results in a large free spectral range (FSR), that is also desirable for filters in wavelength-division-multiplexing applications. For manipulating a beam, the most important task is to regulate the phase front of the transmitted field. Stubs and ring resonators are introduced to regulate the phase retardation at the transmitted field. However, the ring resonator is used to tune the effective refractive index of the MDM slit array. With the adjusting of the parameters of the ring resonator, it is possible to create the suitable phase front needed for beam manipulation. The focal length and bending angle can be controlled, which can be seen from figures 5 and 6. The single stub is used to produce the optical switch effect; the transmission of this structure switches between 'on' and 'off' states with the variation of the length and width of the stub. When one of the slits is in the 'off' state, beam bending and splitting effects can be achieved.

6. Conclusions

In this paper, we have presented novel plasmonic beam manipulation structures consisting of MDM waveguide arrays coupled with stub and circular ring resonators. The propagation characteristics of SPWs have been studied by an

FDTD method. The simulated results clearly show that the deflection angle and the focus position can be controlled easily through the introduction of the stub and the ring resonator. The demonstrated controllability of the radiation direction and focal length, by varying the intensity of light, opens a way to making feasible active plasmonic devices. Compared with existing plasmonic lenses which can bend light, our designs have the advantages of smaller device size, simplicity and ease of integration, indicating promise for finding potential applications in integrated optical circuits, data storage, and so on.

Acknowledgments

[35] Wurtz G A, Pollard R and Zayats A V 2006 Optical bistability in nonlinear surface-plasmon polaritonic crystals *Phys. Rev. Lett.* **97** 057402

[36] Min C J, Wang P, Chen C C, Deng Y, Lu Y H, Ming H, Ning T Y, Zhou Y L and Yang G Z 2008 All-optical switching in subwavelength metallic grating structure containing nonlinear optical materials *Opt. Lett.* **33** 869

[37] Lu H, Liu X M, Gong Y K, Mao D and Wang L R 2011 Optical bistability in metal–insulator–metal plasmonic Bragg waveguides with Kerr nonlinear defects *Appl. Opt.* **50** 1307

[38] Maria A V, Antonella D O, Milan B, Neset A, Mark J B and Michael S 2009 Beam steering from resonant subwavelength slits filled with a nonlinear material *J. Opt. Soc. Am.* B **26** 301

[39] Zheng G G, Chen Y Y, Zhang C Y, Lai M, Su W and Liu Y Z 2012 Beam focusing from double subwavelength metallic slits filled with nonlinear material surrounded by dielectric surface gratings *Photon. Nanostruct.* **10** 560

[40] Pannipitiya A, Rukhlenko I D and Premaratne M 2011 Analytical theory of optical bistability in plasmonic nanoresonators *J. Opt. Soc. Am.* B **28** 2820